

# Validation of the Aeolus L2B wind product by means of airborne wind lidar measurements performed in the North Atlantic region and in the tropics

**Benjamin Witschas(a), Alexander Geiss(b), Oliver Lux(a), Christian Lemmerz(a), Uwe Marksteiner(a), Andreas Schäfler(a), Stephan Rahm(a), Oliver Reitebuch(a), Fabian Weiler(a)**

*(a) German Aerospace Center (Deutsches Zentrum für Luft- und Raumfahrt e.V., DLR), Institute of Atmospheric Physics, Oberpfaffenhofen 82234, Germany*

*(b) Ludwig-Maximilians-University Munich, Meteorological Institute, 80333 Munich, Germany*

**Abstract:** During the first three years of ESA's Aeolus mission, the German Aerospace Center (DLR) conducted four airborne validation campaigns. After having performed two campaigns in Europe (Nov/Dec 2018 and Mai/Jun 2019) the Aeolus VALIDATION Through Airborne LIDARs in Iceland campaign (AVATAR-I) was carried out in the arctic region in Sept/Oct 2019, followed by the campaign in the tropics (AVATAR-T) conducted from Sal, Cape Verde in Sept 2021. During these campaigns, the DLR Falcon aircraft was operated being equipped with two Doppler wind lidar instruments: the ALADIN Airborne Demonstrator (A2D), as the prototype of the direct detection wind lidar instrument on-board Aeolus, and a high-accuracy, coherent detection Doppler wind lidar system (2- $\mu\text{m}$  DWL) that is used as a reference for the Aeolus validation. In this paper, airborne 2- $\mu\text{m}$  DWL observations performed during both the AVATAR-I and AVATAR-T campaign are presented and used to validate the Aeolus L2B wind product and to derive corresponding systematic and random errors in different geographical locations and during different meteorological conditions.

**Keywords:** Aeolus, space-borne wind lidar, coherent wind lidar, direct detection wind lidar.

## 1. Introduction

On 22 August 2018, the first ever spaceborne Doppler wind lidar Aeolus, developed by ESA was launched into space to circle on a sun-synchronous orbit at about 320 km altitude. Since then, Aeolus has been providing profiles of the component of the wind vector along the instrument's line-of-sight (LOS) direction from ground up to about 30 km in the stratosphere [1], primarily aiming to improve numerical weather prediction (NWP) and medium-range weather forecast [2]. Aeolus is carrying a single payload, namely the Atmospheric Laser Doppler Instrument (ALADIN), which is a direct detection wind lidar operating at an ultraviolet wavelength of 354.8 nm. To determine the Doppler shift of the backscattered light from molecules and particles, and with that the LOS wind speed, Aeolus is equipped with two different frequency discriminators, namely a Fizeau interferometer that is used to analyze the frequency shift of the narrowband particulate return signal by means of the so-called fringe imaging technique and two coupled Fabry-Pérot interferometers that are used to analyze the frequency shift of the broadband molecular return signal by the so-called double-edge technique.

The direct detection measurement principle requires regular instrument calibration, a stable instrument alignment and post-processing that relates the measured signal levels to a frequency Doppler shift which can then be translated into a wind speed. This also means that a validation of Aeolus winds by means of independent ground-based and airborne measurements is inevitable to determine the systematic and random errors of the Aeolus wind product but also to improve the wind retrieval algorithms. For that reason, DLR performed four airborne calibration and validation (CalVal) campaigns since the launch of Aeolus. During these campaigns, the DLR Falcon aircraft was equipped with two wind lidar systems. In particular, the Falcon hosted the A2D, which is a prototype of the ALADIN instrument with representative design and measurement principle [3], as well as a coherent detection reference 2- $\mu\text{m}$  DWL with a high sensitivity to particulate returns [4]. Based on these campaign data sets, first insides

in systematic and random errors of the Aeolus L2B wind product have been derived as shown by Lux et al., 2020 [4] and Witschas et al., 2020 [3]. The results shown therein are based on the data set from the first two CalVal campaigns, namely WindVal III (Nov/Dec 2018) and AVATAR-E (May/June 2019).

In this paper, results from the CalVal campaigns AVATAR-I (Sept/Oct 2019) and AVATAR-T (Sept 2021) are presented. The systematic and random errors of the Aeolus wind product are estimated by using 2- $\mu\text{m}$  DWL data. Furthermore, the impact of the different mission time (2019 vs. 2021) and the different campaign regions (North Atlantic vs tropics) on the Aeolus data quality are addressed.

## 2. Validation campaign overview

After having performed two CalVal campaigns in Europe in 2018 and 2019, it was foreseen to extend the CalVal data set to regions where Aeolus is expected to have most significant impact, namely at the polar jet stream, over the oceans, in the lower troposphere and in the tropics [5]. Hence, two further CalVal campaigns, namely the AVATAR-I campaign (Sept/Oct 2019, Keflavik, Iceland) and the AVATAR-T campaign (Sept 2021, Sal, Cape Verde) were performed.

During AVATAR-I, the quality of Aeolus measurements could be investigated in high wind speed regions in the vicinity of the polar jet stream. Furthermore, Aeolus operated with a dedicated range gate setting that was applied exclusively in the area around Iceland during the AVATAR-I time-frame, increasing the overlap of Aeolus and 2- $\mu\text{m}$  DWL data. Altogether, 10 research flights with Aeolus underpasses were conducted during AVATAR-I, covering about 8000 km of the Aeolus measurement track and providing a valuable data set for Aeolus validation in the North Atlantic region. The goal of the AVATAR-T campaign was to validate the Aeolus wind data quality in the tropical region around the Cape Verde archipelago. This operational base allowed to access interesting regions for analyzing for instance the tropical dynamics of the usually Saharan dust-laden African Easterly jet. Altogether, 11 research flights with Aeolus underpasses were conducted, covering about 10600 km of the Aeolus measurement track. An overview of all flight tracks performed within the previously conducted Aeolus CalVal campaigns by DLR is shown in Figure 1.

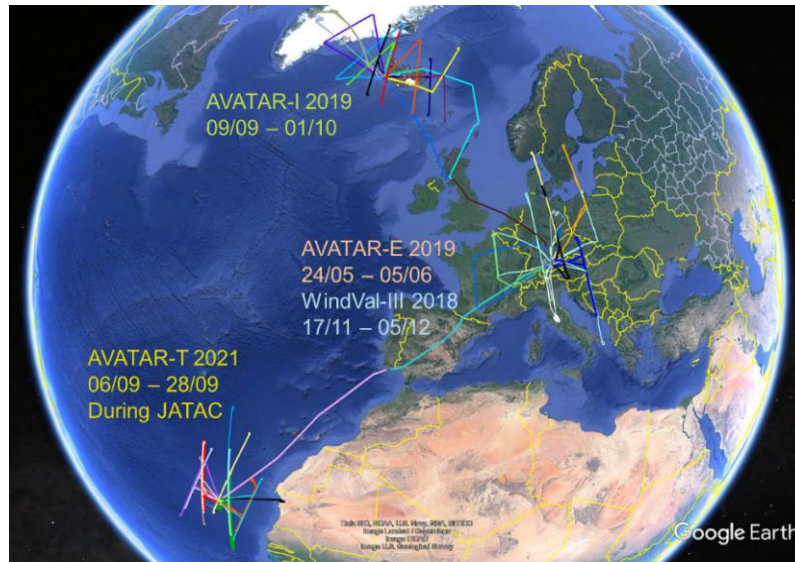


Figure 1. Overview of all flight tracks performed within the previously conducted Aeolus CalVal campaigns by DLR. Each color represents a single flight.

## 3. The Aeolus CalVal payload by DLR

The Aeolus CalVal payload by DLR is composed of two wind lidar systems mounted within DLR's Falcon research aircraft. In particular, the Falcon hosts the A2D which acts as a prototype of the ALADIN instrument with representative design and measurement principle and which is used to investigate particular Aeolus hardware and algorithm topics [3]. On the other hand, the coherent detection 2- $\mu\text{m}$  DWL is used as a reference system due to its very low systematic and random error. In this study, only data from the 2- $\mu\text{m}$  DWL are discussed.

The 2- $\mu$ m DWL is a coherent detection wind lidar system based on a Tm:LuAG laser operating at a wavelength of 2022.54 nm (vacuum), a laser pulse energy of 1 to 2 mJ and a pulse repetition rate of 500 Hz, ensuring eye-safe operation. The system was built by CLR Photonics, Inc. and has been deployed at DLR since October 1999. The 2- $\mu$ m DWL is composed of three units, namely (1) a transceiver head containing the laser, a 11 cm afocal telescope, receiver optics, detectors and a double-wedge scanner; (2) a power supply and the cooling unit of the laser; and (3) a rack containing the data acquisition unit and the control electronics, developed by DLR (further details can be found in [6]).

#### 4. Comparison of Aeolus and 2- $\mu$ m Doppler wind lidar data

Due to the different horizontal and vertical resolutions of 2- $\mu$ m DWL measurements ( $\approx 8.4$  km, 100 m for one scanner revolution) and Aeolus measurements ( $\approx 90$  km (Rayleigh) and down to  $\approx 10$  km (Mie), 0.25 to 2 km), averaging procedures are needed in order to compare respective wind observations. Furthermore, as Aeolus only provides HLOS winds, the 2- $\mu$ m DWL measurements have to be projected onto the Aeolus HLOS direction. This procedure is illustrated by means of the Aeolus underflight performed on 16 Sept 2019 during the AVATAR-I campaign as shown in Figure 2.

First, the wind speed (Figure 2, top left) and wind direction (Figure 2, top right) measured by the 2- $\mu$ m DWL are averaged to the Aeolus grid by using the top and bottom altitudes as well as the start and stop latitudes given in the Aeolus Level 2B data product. Afterwards, all valid averaged wind speeds and directions are projected onto the horizontal LOS of Aeolus by using the range-dependent azimuth angle (Figure 2, bottom left). In a next step, the Aeolus HLOS winds are extracted for areas of valid 2- $\mu$ m DWL measurements. Beforehand, the data are filtered by means of an estimated error for the wind speeds. In this study, a threshold for the estimated error of 7.0 m/s (Ray) and 5.5 m/s (Mie) was used for the AVATAR-I data set, and 8.5 m/s (Ray) and 5.0 m/s (Mie) for the AVATAR-T data set.

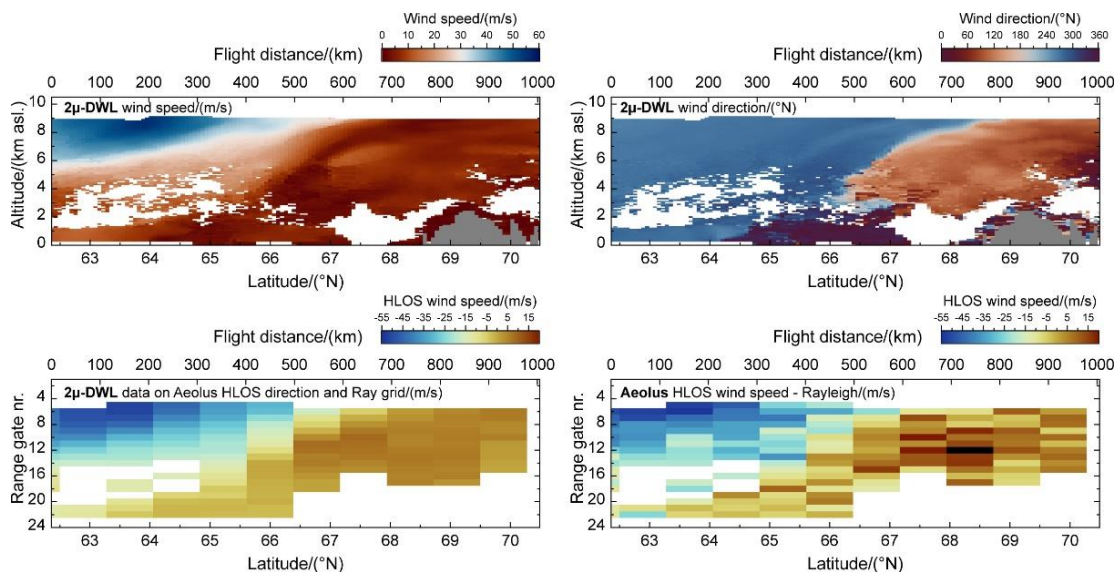


Figure 2. 2- $\mu$ -DWL wind speed (top, left) and wind direction (top, right) for the AVATAR-I underflight on 16 Sept 2019. The corresponding 2- $\mu$ -DWL projection onto the Aeolus HLOS direction is shown in the bottom left, whereas the Aeolus HLOS Rayleigh winds are shown in the bottom right.

#### 5. Discussions

In Figure 3, Rayleigh-clear winds and Mie-cloudy winds are indicated by blue dots and orange dots, respectively. Line fits to the corresponding data sets are depicted by the light blue and the yellow lines. The  $x = y$  line is represented by the gray dashed line.

Altogether, the 10 satellite underflights during the AVATAR-I campaign resulted in 1155 data points for Rayleigh-clear wind validation and 701 data points for Mie-cloudy wind validation, whereas 18 (Rayleigh-clear) and 30 (Mie-cloudy) data points are treated as outliers as they exceed a modified Z-score threshold of 3. The 11 underflights during AVATAR-T provided 439 (Rayleigh-clear) and 132 (Mie-cloudy) data points for comparison, with 11 outliers for Rayleigh-clear and 9 for Mie-cloudy

winds. The significant reduction of data points was due to a degrading 2- $\mu$ m DWL performance during the campaign's duration, caused by the high temperature and humidity gradients that induced a misalignment of the transceiver unit as well as a non-optimized Aeolus range gate setting during the AVATAR-T campaign.

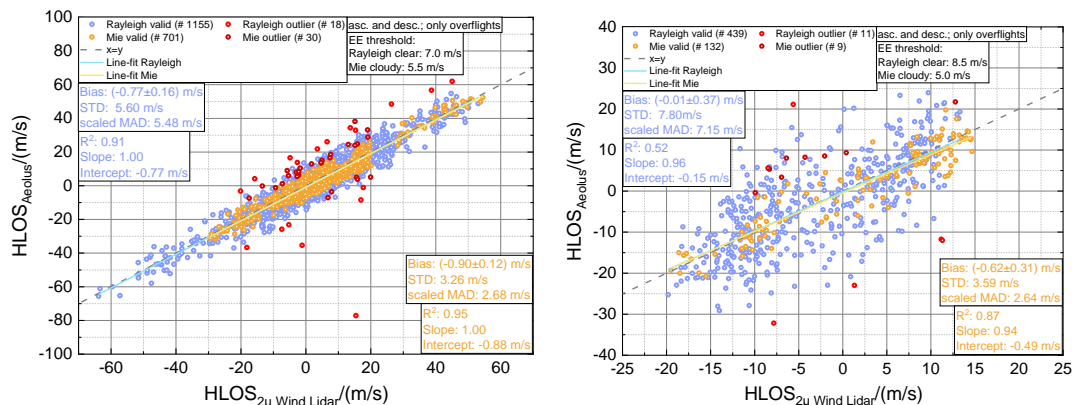


Figure 3. Aeolus HLOS wind speed plotted against the 2- $\mu$ m DWL wind speed projected onto the horizontal viewing direction of Aeolus for all underflights performed during AVATAR-I (left) and AVATAR-T (right). The wind measurements are separated in Rayleigh-clear winds (blue) and Mie-cloudy winds (orange), outliers indicated by a modified Z-score larger than 3 are indicated in red.

It can be seen that Aeolus and 2- $\mu$ m DWL data are in great accordance, although the spread is larger for the AVATAR-T data set. This mainly has to do with the fact, that the overall signal levels during the AVATAR-T period were only about half of the one acquired during AVATAR-I, caused by a degrading Aeolus instrument performance. Fortunately, on the other hand, the solar background signal during AVATAR-T was about a factor of 3 smaller compared to AVATAR-I, partly compensating the negative impact of the reduced signal levels on the determined random error.

In particular, the determined systematic error for Rayleigh clear winds is  $(-0.8 \pm 0.2)$  m/s (AVATAR-I) and  $(0.0 \pm 0.4)$  m/s (AVATAR-T). The one for Mie-cloudy winds is  $(-0.9 \pm 0.1)$  m/s (AVATAR-I) and  $(-0.6 \pm 0.3)$  m/s (AVATAR-T). Hence, for both campaign periods and both wind products, the mission goal of a systematic error below 0.7 m/s is almost met. The random error for Rayleigh-clear winds, represented by the scaled MAD, is determined to be 5.5 m/s (AVATAR-I) and 7.2 m/s (AVATAR-T), whereas the significant increase is caused by the lower return signal levels during AVATAR-T. For the Mie-cloudy winds, the random error is 2.7 m/s (AVATAR-I) and 2.6 m/s (AVATAR-T) and hence, almost identical, as the Mie return signal is not only depending on the alignment of the instrument but also on the overall particle content in the atmosphere which was larger during AVATAR-T.

## 6. References

- [1] ESA, “The four candidate Earth explorer core missions: Atmospheric dynamics mission”, ESA Report for Mission Selection, ESA, SP-1233, 145 pp., (1999).
- [2] A. Horányi, C. Cardinali, M. Rennie, L. Isaksen, “The assimilation of horizontal line-of-sight wind information into the ECMWF data assimilation and forecasting system. Part I: The assessment of wind impact”, Q. J. Roy. Meteor. Soc., 141, 1223-1232, (2015).
- [3] O. Lux, C. Lemmerz, F. Weiler, U. Marksteiner, B. Witschas, S. Rahm, A. Geiß, O. Reitebuch, “Intercom Intercomparison of wind observations from the European Space Agency’s Aeolus satellite mission and the ALADIN Airborne Demonstrator”, Atmos. Meas. Tech., 13, 2075–2097 (2020).
- [4] B. Witschas, C. Lemmerz, A. Geiß, A., O. Lux, U. Marksteiner, S. Rahm, O. Reitebuch, F. Weiler, “First validation of Aeolus wind observations by airborne Doppler wind lidar measurements, Atmos. Meas. Tech., 13, 2381–2396 (2020).
- [5] DGH Tan and E. Anderson, “Simulation of the yield and accuracy of wind profile measurements from the Atmospheric Dynamics Mission (ADM-Aeolus). Q. J. R. Meteorol. Soc. 131: 1737–1757 (2005).
- [6] B. Witschas, S. Rahm, A. Dörnbrack, J. Wagner, M. Rapp, „Airborne wind lidar measurements of vertical and horizontal winds for the investigation of orographically gravity waves“, J. Atmos. Ocean. Tech., 34, 1371–1386, (2017).